Measurement of the form-factor ratios for $D^+ \to \overline{K}^{\star 0}\ell^+\nu_\ell$

E. M. Aitala,[9] S. Amato,[1] J. C. Anjos,[1] J. A. Appel,[5] D. Ashery,[14] S. Banerjee,[5] I. Bediaga,[1] G. Blaylock,[8] S. B. Bracker,[15] P. R. Burchat,[13] R. A. Burnstein,[6] T. Carter,[5] H. S. Carvalho,[1] N. K. Copty,[12] L. M. Cremaldi,[9] C. Darling,[18] K. Denisenko,[5] A. Fernandez,[11] G.F. Fox,[12] P. Gagnon,[2] C. Gobel,[1] K. Gounder,[9] A. M. Halling,[5] G. Herrera,[4] G. Hurvits,[14] C. James,[5] P. A. Kasper,[6] S. Kwan,[5] D. C. Langs,[12] J. Leslie,[2] B. Lundberg,[5] S. MayTal-Beck,[14] B. Meadows,[3] J. R. T. de Mello Neto,[1] D. Mihalcea,[7] R. H. Milburn,[16] J. M. de Miranda,[1] A. Napier,[16] A. Nguyen,[7] A. B. d'Oliveira,[3,11] K. O'Shaughnessy,[2] K. C. Peng,[6] L. P. Perera,[3] M. V. Purohit,[12] B. Quinn,[9] S. Radeztsky,[17] A. Rafatian,[9] N. W. Reay,[7] J. J. Reidy,[9] A. C. dos Reis,[1] H. A. Rubin,[6] D. A. Sanders,[9] A. K. S. Santha,[3] A. F. S. Santoro,[1] A. J. Schwartz,[3] M. Sheaff,[17] R. A. Sidwell,[7] A. J. Slaughter,[18] M. D. Sokoloff,[3] J. Solano,[1] N. R. Stanton,[7] R. J. Stefanski,[5] K. Stenson,[17] D. J. Summers,[9] S. Takach,[18] K. Thorne,[5] A. K. Tripathi,[7] S. Watanabe,[17] R. Weiss-Babai,[14] J. Wiener,[10] N. Witchey,[7] E. Wolin,[18] D. Yi,[9] S. M. Yang,[7] S. Yoshida,[7] R. Zaliznyak,[13] and C. Zhang[7]

(Fermilab E791 Collaboration)

[1] *Centro Brasileiro de Pesquisas Físicas, Rio de Janeiro, Brazil*
[2] *University of California, Santa Cruz, California 95064*
[3] *University of Cincinnati, Cincinnati, Ohio 45221*
[4] *CINVESTAV, Mexico*
[5] *Fermilab, Batavia, Illinois 60510*
[6] *Illinois Institute of Technology, Chicago, Illinois 60616*
[7] *Kansas State University, Manhattan, Kansas 66506*
[8] *University of Massachusetts, Amherst, Massachusetts 01003*
[9] *University of Mississippi, University, Mississippi 38677*
[10] *Princeton University, Princeton, New Jersey 08544*
[11] *Universidad Autonoma de Puebla, Mexico*
[12] *University of South Carolina, Columbia, South Carolina 29208*
[13] *Stanford University, Stanford, California 94305*
[14] *Tel Aviv University, Tel Aviv, Israel*
[15] *Box 1290, Enderby, BC, V0E 1V0, Canada*
[16] *Tufts University, Medford, Massachusetts 02155*
[17] *University of Wisconsin, Madison, Wisconsin 53706*
[18] *Yale University, New Haven, Connecticut 06511*

September 14, 1998

The form factor ratios $r_V = V(0)/A_1(0)$, $r_2 = A_2(0)/A_1(0)$ and $r_3 = A_3(0)/A_1(0)$ in the decay $D^+ \to \overline{K}^{\star 0}\ell^+\nu_\ell$, $\overline{K}^{\star 0} \to K^-\pi^+$ have been measured using data from charm hadroproduction experiment E791 at Fermilab. From 3034 (595) signal (background) events in the muon channel, we obtain $r_V = 1.84 \pm 0.11 \pm 0.09$, $r_2 = 0.75 \pm 0.08 \pm 0.09$ and, as a first measurement of r_3, we find $0.04 \pm 0.33 \pm 0.29$. The values of the form factor ratios r_V and r_2 measured for the muon channel are combined with the values of r_V and r_2 that we have measured in the electron channel. The combined E791 results for the muon and electron channels are $r_V = 1.87 \pm 0.08 \pm 0.07$ and $r_2 = 0.73 \pm 0.06 \pm 0.08$.

13.20.Fc,14.40.Lb

The weak decays of hadrons containing heavy quarks are substantially influenced by strong interaction effects. Semileptonic charm decays such as $D^+ \to \overline{K}^{\star 0}\ell^+\nu_\ell$ are an especially clean way to study these effects because the leptonic and hadronic currents completely factorize in the decay amplitude. All information about the strong interactions can be parametrized by a few form factors. Also, according to Heavy Quark Effective Theory, the values of form factors for some semileptonic charm decays can be related to those governing certain b-quark decays. In particular, the form factors studied here can be related to those for the rare B–meson decays $B \to K^\star e^+e^-$ and $B \to K^\star\gamma$ [1,2] which provide windows for physics beyond the Standard Model.

With a vector meson in the final state, there are four form factors, $V(q^2)$, $A_1(q^2)$, $A_2(q^2)$ and $A_3(q^2)$, which are functions of the Lorentz-invariant momentum transfer squared [3]. The differential decay rate for $D^+ \to \overline{K}^{*0}\mu^+\nu_\mu$ with $\overline{K}^{*0} \to K^-\pi^+$ is a quadratic homogeneous function of the four form factors. Unfortunately, the limited size of current data samples precludes precise measurement of the q^2-dependence of the form factors; we thus assume the dependence to be given by the nearest-pole dominance model: $F(q^2) = F(0)/(1 - q^2/m_{pole}^2)$ where $m_{pole} = m_V = 2.1\ \mathrm{GeV}/c^2$ for the vector form factor V, and $m_{pole} = m_A = 2.5\,\mathrm{GeV}/c^2$ for the three axial-vector form factors [4]. The third form factor $A_3(q^2)$, which is unobservable in the limit of vanishing lepton mass, probes the spin-0 component of the off-shell W. Additional spin-flip amplitudes, suppressed by an overall factor of m_ℓ^2/q^2 when compared with spin no-flip amplitudes, contribute to the differential decay rate. Because $A_1(q^2)$ appears among the coefficients of every term in the differential decay rate, it is customary to factor out $A_1(0)$ and to measure the ratios $r_V = V(0)/A_1(0)$, $r_2 = A_2(0)/A_1(0)$ and $r_3 = A_3(0)/A_1(0)$. The values of these ratios can be extracted without any assumption about the total decay rate or the weak mixing matrix element V_{cs}.

We report new measurements of the form factor ratios for the muon channel and combine them with slightly revised values of our previously published measurements of r_V and r_2 [5] for the electron channel. This is the first set of measurements in both muon and electron channels from a single experiment. We also report the first measurement of $r_3 = A_3(0)/A_1(0)$, which is unobservable in the limit of vanishing charged lepton mass.

E791 is a fixed-target charm hadroproduction experiment [6]. Charm particles were produced in the collisions of a 500 GeV/c π^- beam with five thin targets, one platinum and four diamond. About 2×10^{10} events were recorded during the 1991-1992 Fermilab fixed-target run. The tracking system consisted of 23 planes of silicon microstrip detectors, 45 planes of drift and proportional wire chambers, and two large-aperture dipole magnets. Hadron identification is based on the information from two multicell Čerenkov counters that provided good discrimination between kaons and pions in the momentum range $6 - 36\ \mathrm{GeV}/c$. In this momentum range, the probabability of misidentifying a pion as a kaon depends on momentum but does not exceed 5%. We identified muon candidates using a single plane of scintillator strips, oriented horizontally, located behind an equivalent of 2.4 meters of iron (comprising the calorimeters and one meter of bulk steel shielding). The angular acceptance of the scintillator plane was $\approx \pm 62$ mrad $\times$ ± 48 mrad (horizontally and vertically, respectively), which is somewhat smaller than that of the rest of the spectrometer for tracks which go through both magnets ($\approx \pm 100$ mrad $\times$ ± 64 mrad). The vertical position of a hit was determined from the strip's vertical position, and the horizontal position of a hit from timing information.

The event selection criteria used for this analysis are the same as for the electronic-mode form factor analysis [5], except for those related to lepton identification. Events are selected if they contain an acceptable decay vertex determined by the intersection point of three tracks that have been identified as a muon, a kaon, and a pion. The longitudinal separation between this candidate decay vertex and the reconstructed production vertex is required to be at least 15 times the estimated error on the separation. The two hadrons must have opposite charge. If the kaon and the muon have opposite charge, the event is assigned to the "right-sign" sample; if they have the same charge, the event is assigned to the "wrong-sign" sample used to model the background.

To reduce the contamination from hadron decays in flight, only muon candidates with momenta larger than 8 GeV/c are retained. With this momentum restriction, the efficiency of muon tagging was about 85%, and the probability for a hadron to be identified as a muon was about 3%.

To exclude feedthrough from $D^+ \to K^-\pi^+\pi^+$, we exclude events in which the invariant mass of the three charged particles (with the muon candidate interpreted as a pion) is consistent with the D^+ mass. For our final selection criteria, we use a binary-decision-tree algorithm (CART [7]), which finds linear combinations of parameters that have the highest discrimination power between signal and background. Using this algorithm, we found a linear combination of four discrimination variables [5]: (a) separation significance of the candidate decay vertex from target material; (b) distance of closest approach of the candidate D momentum vector to the primary vertex, taking into account the maximum kinematically-allowed miss distance due to the unobserved neutrino; (c) product over candidate D decay tracks of the distance of closest approach of the track to the secondary vertex, divided by the distance of closest approach to the primary vertex, where each distance is measured in units of measurement errors; and (d) significance of separation between the production and decay vertices. This final selection criterion reduced the number of wrong-sign events by 50%, and the number of right-sign events by 25%. Although this does not affect our sensitivity substantially, it does reduce systematic uncertainties associated with the background subtraction.

The minimum parent mass M_{min} is defined as the invariant mass of $K\pi\mu\nu$ when the neutrino momentum component along the D^+ direction of flight is ignored. The distribution of M_{min} should have a Jacobian peak at the D^+ mass, and we observe such a peak in our data (Fig. 1). We retain events with M_{min} in the range 1.6 to 2.0 GeV/c^2 as indicated by the arrows in the figure. The distribution of $K\pi$ invariant mass for the retained events is shown in the top right of Fig. 1 for both right-sign and wrong-sign samples. Candidates with $0.85 < M_{K\pi} < 0.94$ GeV/c^2 were retained, yielding final data samples of 3629 right-sign and 595 wrong-sign events.

The hadroproduction of charm, the differential decay rate, and the detector response were simulated with a Monte Carlo event generator. A sample of events was generated according to the differential decay rate (Eq. 22 in Ref. [3]), with the form factor ratios $r_V = 2.00$, $r_2 = 0.82$, and $r_3 = 0.00$. The same selection criteria were applied to the Monte Carlo events as to real data. Out of 25 million generated events, 95579 decays passed all cuts. Figure 1 (bottom) shows the distribution of $M_{K\pi}$ from real data after background subtraction ("right-sign" minus "wrong-sign") overlaid with the corresponding Monte Carlo distribution after all cuts are applied. The agreement between the two distributions suggests that wrong-sign events correctly account for the size of the background.

The differential decay rate [3] is expressed in terms of four independent kinematic variables: the square of the momentum transfer (q^2), the polar angle θ_V in the $\overline{K}^{\star 0}$ rest frame between the π^+ and D^+, the polar angle θ_ℓ in the W^+ rest frame between the ν_μ and D^+, and the azimuthal angle χ in the D^+ rest frame between the $\overline{K}^{\star 0}$ and W^+ decay planes. The definition we use for the polar angle θ_ℓ is related to the definition used in Ref. [3] by $\theta_\ell \rightarrow \pi - \theta_\ell$.

Semileptonic decays cannot be fully reconstructed due to the undetected neutrino. With the available information about the D^+ direction of flight and the charged daughter particle momenta, the neutrino momentum (and all the decay's kinematic variables) can be determined up to a two-fold ambiguity if the parent mass is constrained. Monte Carlo studies show that the differential decay rate is more accurately determined if it is calculated with the solution corresponding to the lower laboratory-frame neutrino momentum.

To extract the form factor ratios the distribution of the data points in the four-dimensional kinematic variable space is fit to the full expression for the differential decay rate. We use the same unbinned maximum-likelihood fitting technique as in our $D^+ \rightarrow \overline{K}^{\star 0} e^+ \nu_e$ form factor analysis [5]. The likelihood function is computed from the density of weighted Monte Carlo events (described above) near each data event in the four-dimensional space of kinematic variables [8]. To include background in the fit, a similar likelihood function based on the density of wrong-sign events around each right-sign event is used. With this method the fitted results are subject to small systematic biases which originate from two sources: (a) approximate normalization of the likelihood function; (b) nonlinearity of the decay rate within the volume centered on the data point. These systematic biases of the fitted parameters were determined from Monte Carlo studies, and are $\delta r_V = +0.09 \pm 0.02$, $\delta r_2 = -0.08 \pm 0.01$ and $\delta r_3 = -0.11 \pm 0.06$. After correction for these biases by subtracting these δr's from the measured values, the final form factor ratios and their statistical errors are

$r_V = 1.84 \pm 0.11$, $r_2 = 0.75 \pm 0.08$ and $r_3 = 0.04 \pm 0.33$. The sensitivity of the fit to r_3 is low because this form factor ratio only contributes to spin-flip amplitudes. The correlation coefficient between the form factors to which we are most sensitive, r_V and r_2, is -0.090. The correlation coefficient between r_3 and r_2 is -0.211, and between r_3 and r_V is -0.087. Figure 2 compares the data and Monte Carlo distributions in various regions of the four-dimensional phase space.

We checked for any potential bias in these results due to our choice of neutrino momentum by employing a secondary fitting technique. Again, Monte Carlo is used to account for detector acceptance and smearing. However, both solutions for the neutrino momentum are now used in the fit. We divide the four-dimensional kinematic variable space into 240 separate volumes and determine the number of data entries in each volume, where each event has two entries – one for each neutrino-momentum solution. We use Monte Carlo events to determine the probabilities that an event generated in a particular phase space volume will be observed in each of the other volumes when the wrong neutrino-momentum choice is used. This feedthrough probability matrix and the observed number of data events determine the fraction of data events that correspond to the correct neutrino-momentum solution in each volume of kinematic variable space. Each fraction is then used in a binned maximum likelihood fit. Background is modeled with wrong-sign candidates as in the primary method. The form factor ratios and statistical errors measured with this secondary method are $r_V = 1.90 \pm 0.11$, $r_2 = 0.72 \pm 0.08$, and $r_3 = -0.25 \pm 0.34$. This method for extracting the form factor ratios uses the same $D^+ \to \overline{K}^{*0} \mu^+ \nu_\mu$ candidates as the previous method, but uses additional neutrino-momentum solutions. This is true for both the data and for the Monte Carlo sample used in the likelihood function calculation, so the results of this fit could differ from those of the previous fit.

The values of the form factor ratios obtained with the two methods agree well, providing further assurance that selecting the lower neutrino momentum solution in the primary method and correcting for the systematic bias gives the correct result. However, the systematic uncertainties for the primary method (see below) were found to be significantly smaller, mainly because the unbinned maximum-likelihood method is more stable against changes in the size of the phase space volume. Therefore, the primary method was chosen for quoting final results.

We classify systematic uncertainties into three categories: (a) Monte Carlo simulation of detector effects and production mechanism; (b) fitting technique; (c) background subtraction. The estimated contributions of each are given in Table I. The main contributions to category (a) are due to muon identification and data selection criteria. The contributions to category (b) are related to the limited size of the Monte Carlo sample and to corrections for systematic bias.

The measurements of the form factor ratios for $D^+ \to \overline{K}^{*0}\mu^+\nu_\mu$ presented here and for the similar decay channel $D^+ \to \overline{K}^{*0}e^+\nu_e$ [5] follow the same analysis procedure except for the charged lepton identification. Both results are listed in Table II. The consistency within errors of the results measured in the electron and muon channels supports the assumption that strong interaction effects, incorporated in the values of form factor ratios, do not depend on the particular W^+ leptonic decay. Based on this assumption, we combine the results measured for the electronic and muonic decay modes. The averaged values of the form factor ratios are $r_V = 1.87 \pm 0.08 \pm 0.07$ and $r_2 = 0.73 \pm 0.06 \pm 0.08$. The statistical and systematic uncertainties of the average results were determined using the general procedure described in Ref. [9] (Eqns. 3.40 and 3.40′). Some of the systematic errors for the two samples have positive correlation coefficients, and some negative. The combination of all systematic errors is ultimately close to that which one would obtain assuming all the errors are uncorrelated. The third form factor ratio r_3 was not measured in the electronic mode.

Table II compares the values of the form factor ratios r_V and r_2 measured by E791 in the electron, muon and combined modes with previous experimental results. The size of the data sample and the decay channel are listed for each case. All experimental results are consistent within errors. The comparison between the E791 combined values of the form factor ratios r_V and r_2 and previous experimental results is also shown in Fig. 3 (top). Table III and Fig. 3 (bottom) compare the final E791 result with published theoretical predictions. The spread in the theoretical results is significantly larger than the E791 experimental errors.

To summarize, we have measured the values of the form factor ratios in the decay channel $D^+ \to \overline{K}^{*0}\mu^+\nu_\mu$ to be $r_V = 1.84 \pm 0.11 \pm 0.09$, $r_2 = 0.75 \pm 0.08 \pm 0.09$ and $r_3 = 0.04 \pm 0.33 \pm 0.29$. The data sample has about 3000 events after subtracting 595 background events. Combining these results for r_V and r_2 with those measured by E791 for the decay channel $D^+ \to \overline{K}^{*0}e^+\nu_e$ gives $r_V = 1.87 \pm 0.08 \pm 0.07$ and $r_2 = 0.73 \pm 0.06 \pm 0.08$.

We gratefully acknowledge the assistance from Fermilab and other participating institutions. This work was supported by the Brazilian Conselho Nacional de Desenvolvimento Científico e Technológico, CONACyT (Mexico), the Israeli Academy of Sciences and Humanities, the U.S. Departament of Energy, the U.S.-Israel Binational Science Foundation, and the U.S. National Science Foundation.

[1] N. Isgur and M. B. Wise, Phys. Rev. D 42 (1990) 2388.

[2] Z. Ligeti, I. W. Stewart and M. B. Wise, Phys. Lett. B 420 (1998) 359.
[3] J.G. Körner and G.A. Schuler, Phys. Lett. B 226 (1989) 185.
[4] Particle Data Group, Review of Particle Physics, Phys. Rev. D 50 (1994) 1568.
[5] Fermilab E791 Collaboration , E.M. Aitala et al., Phys. Rev. Lett. 80 (1998) 1393. The E791 electron result for r_V quoted in this paper is 0.06 higher than the value reported in this reference because we have corrected for inaccuracies in the earlier modeling of the D^+ transverse momentum.
[6] J.A. Appel, Ann. Rev. Nucl. Part. Sci. 42 (1992) 367; D.J. Summers et al., XXVII Rencontre de Moriond, Les Arcs, France (15-22 March 1992) 417.
[7] L. Brieman et al., Classification and Regression Trees (Chapman and Hall, New York, 1984).
[8] D.M. Schmidt, R.J. Morrison, and M.S. Witherell, Nucl. Instrum. Methods A 328 (1993) 547.
[9] L. Lyons, Statistics for Nuclear and Particle Physicists (Cambridge University Press, Cambridge, 1986).
[10] Fermilab E687 Collaboration, P.L. Frabetti et al., Phys. Lett. B 307 (1993) 262.
[11] Fermilab E653 Collaboration, K. Kodama et al., Phys. Lett. B 274 (1992) 246.
[12] Fermilab E691 Collaboration, J.C. Anjos et al., Phys. Rev. Lett. 65 (1990) 2630.
[13] D. Scora and N. Isgur, Phys. Rev. D 52 (1995) 2783. We have used the q^2-dependence assumed in the fits to data to extrapolate the theoretical form factors from $q^2 = q^2_{max}$ to $q^2 = 0$.
[14] M. Wirbel, B. Stech, and M. Bauer, Z. Phys. C 29 (1985) 637.
[15] T. Altomari and L. Wolfenstein, Phys. Rev. D 37 (1988) 681.
[16] F.J. Gilman and R.L. Singleton, Jr., Phys. Rev. D 41 (1990) 142.
[17] B. Stech, Z. Phys. C 75 (1997) 245.
[18] C.W. Bernard, Z.X. El-Khadra, and A. Soni, Phys. Rev. D 45 (1992) 869, Phys. Rev. D 47 (1993) 998.
[19] V. Lubicz, G. Martinelli, M. S. McCarthy, and C. T. Sachrajda, Phys. Lett. B 274 (1992) 415.
[20] A. Abada et al., Nucl. Phys. B 416 (1994) 675.
[21] C.R. Alton et al., Phys. Lett. B 345 (1995) 513.
[22] K. C. Bowler et al., Phys. Rev. D 51 (1995) 4905.
[23] P. Ball, V.M. Braun, and H.G. Dosch, Phys. Rev. D 44 (1991) 3567.
[24] T. Bhattacharya and R. Gupta, Nucl. Phys. B (Proc. Suppl.) 47 (1996) 481.

TABLE I. The main contributions to uncertainties on the form factor ratios.

Source	σ_{r_2}	σ_{r_V}	σ_{r_3}
Simulation of detector effects:	0.06	0.08	0.16
Hadron identification	0.01	0.01	0.02
Muon identification	0.04	0.06	0.10
Production mechanism	0.01	0.01	0.02
Acceptance	0.03	0.02	0.08

Cut selection	0.03	0.04	0.09
Fitting technique:	0.02	0.03	0.22
MC volume size	0.02	0.02	0.12
Number of MC points	0.01	0.01	0.18
Bias	0.01	0.02	0.06
Background:	0.06	0.04	0.08
No. of background events	0.04	0.02	0.06
Background shape	0.04	0.04	0.06
Total	0.09	0.09	0.29

TABLE II. Comparison of E791 results with previous experimental results. The E791 electron result for r_V is 0.06 higher than the value reported in Ref. [5] because we have corrected for inaccuracies in the earlier modeling of the D^+ transverse momentum.

Exp.	Events	$r_V = V(0)/A_1(0)$	$r_2 = A_2(0)/A_1(0)$
E791	6000 $(e+\mu)$	$1.87 \pm 0.08 \pm 0.07$	$0.73 \pm 0.06 \pm 0.08$
E791	3000 (μ)	$1.84 \pm 0.11 \pm 0.09$	$0.75 \pm 0.08 \pm 0.09$
E791	3000 (e)	$1.90 \pm 0.11 \pm 0.09$	$0.71 \pm 0.08 \pm 0.09$
E687 [10]	900 (μ)	$1.74 \pm 0.27 \pm 0.28$	$0.78 \pm 0.18 \pm 0.10$
E653 [11]	300 (μ)	$2.00^{+0.34}_{-0.32} \pm 0.16$	$0.82^{+0.22}_{-0.23} \pm 0.11$
E691 [12]	200 (e)	$2.0 \pm 0.6 \pm 0.3$	$0.0 \pm 0.5 \pm 0.2$

TABLE III. Comparison of E791 results with theoretical predictions for the form factor ratios r_V and r_2.

Group	r_V	r_2
E791 (e and μ)	1.87 ± 0.11	0.73 ± 0.10
ISGW2 [13]	2.0	1.3
WSB [14]	1.4	1.3
KS [3]	1.0	1.0
AW/GS [15,16]	2.0	0.8
Stech [17]	1.55	1.06
BKS [18]	$1.99 \pm 0.22 \pm 0.33$	$0.7 \pm 0.16 \pm 0.17$
LMMS [19]	1.6 ± 0.2	0.4 ± 0.4
ELC [20]	1.3 ± 0.2	0.6 ± 0.3
APE [21]	1.6 ± 0.3	0.7 ± 0.4
UKQCD [22]	$1.4^{+0.5}_{-0.2}$	0.9 ± 0.2
BBD [23]	2.2 ± 0.2	1.2 ± 0.2
LANL [24]	1.78 ± 0.07	0.68 ± 0.11

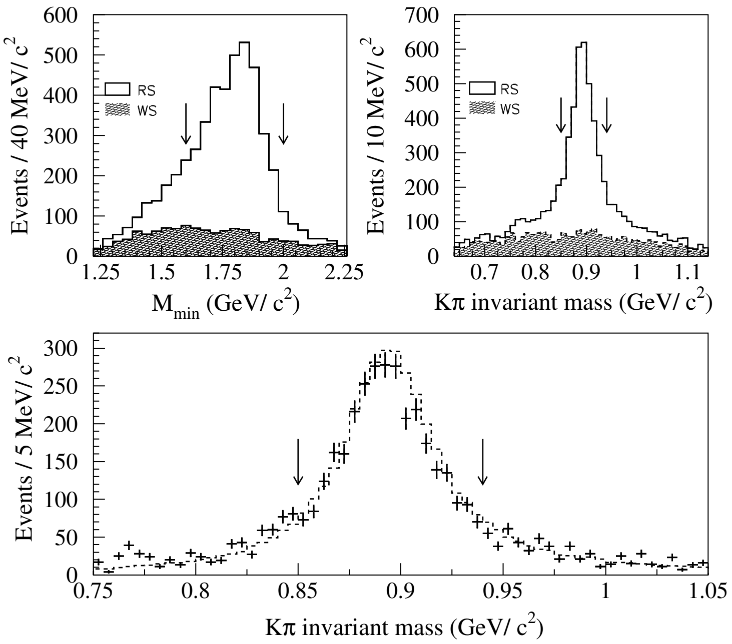

FIG. 1. Distributions of minimum parent mass M_{min} and $K\pi$ invariant mass for $D^+ \to \overline{K}^{*0}\mu^+\nu_\mu$ candidate events. Right-sign (RS) and wrong-sign (WS) samples are defined in the text. Top left: M_{min} for events with $K\pi$ mass in the range 0.85 to 0.94 GeV$/c^2$. Top right: $K\pi$ invariant mass for events with M_{min} in the range 1.6 to 2.0 GeV$/c^2$. Bottom: background-subtracted (RS-WS) $K\pi$ mass distribution (crosses) compared to Monte Carlo prediction (dashed histogram) for events with M_{min} in the range 1.6 to 2.0 GeV$/c^2$. All candidates pass all the other final selection cuts. The arrows indicate the range of the final sample.

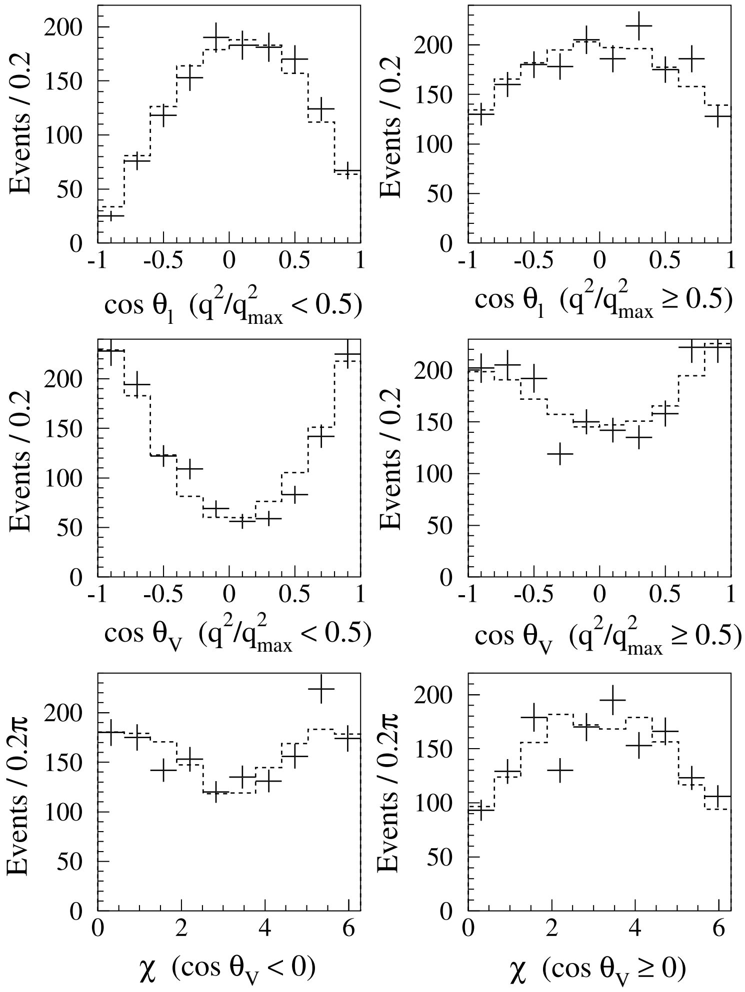

FIG. 2. Comparison of single-variable distributions of background-subtracted data (crosses) with Monte Carlo predictions (dashed histograms) using best-fit values for the form factor ratios.

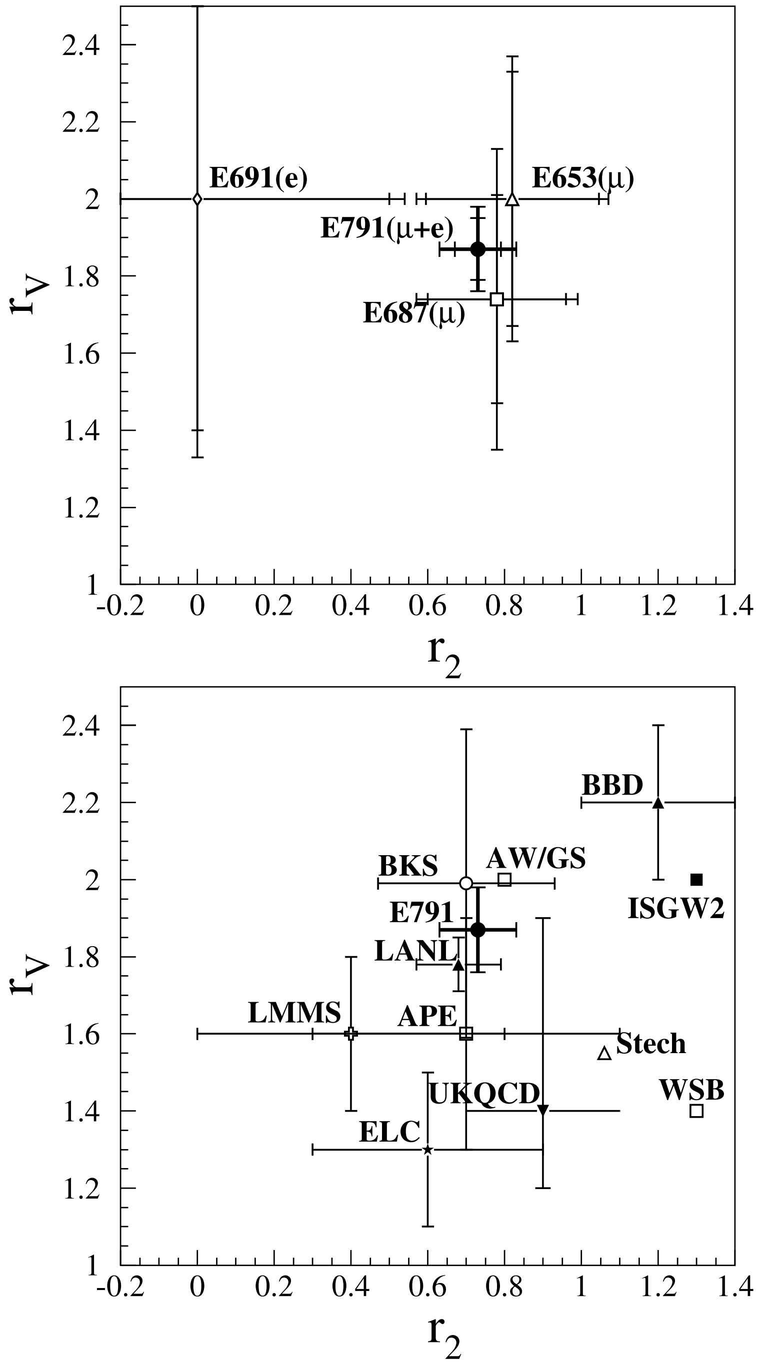

FIG. 3. Top: Comparison of experimental measurements of form factor ratios r_V and r_2 for $D^+ \to \overline{K}^{*0}\ell^+\nu_\ell$ in the muon (μ), electron (e) and combined ($\mu+e$) channels. The smaller error bars indicate the statistical errors and the larger ones indicate the statistical and sytematic errors added in quadrature. Bottom: Comparison of theoretical predictions with the E791 ($\mu+e$) result.